QED contribution to J/ψ production with light hadrons at B factories

Zhi-Guo He[1] and Jian-Xiong Wang[2,3]

[1] *II. Institut für Theoretische Physik, Universität Hamburg, Luruper Chaussee 149, 22761 Hamburg, Germany*

[2] *Institute of High Energy Physics, Chinese Academy of Science, P.O. Box 918(4), Beijing, 100049, China and Theoretical Physics Center for Science Facilities (CAS), Beijing, 100049, China*

[3] *School of Physical Sciences, University of Chinese Academy of Sciences, Beijing, 100049, China*

(Received 21 March 2013; revised manuscript received 29 April 2019; published 16 December 2019)

To understand the $J/\psi + X_{\text{non-}c\bar{c}}$ production mechanism in e^+e^- annihilation, in this work, we propose to measure the cross section for J/ψ production without the association of a charm quark pair without any constraint on the number of charged tracks in the final state events except for the $\mu^+\mu^-$ from J/ψ decay, which we will refer to here as J/ψ production with light hadrons at B factories. We also present a detailed study on its QED background due to $\psi(2S)$ feed-down, where the $\psi(2S)$ is produced through $e^+e^- \to \psi(2S) + \gamma$ and $e^+e^- \to \psi(2S) + f\bar{f}$ ($f =$ lepton, light quark), as well as those due to the QED contribution to the direct $J/\psi + q\bar{q}$ production with $q = u$, d, s quark. We find that the QED background is huge in the whole phase space region; however, it can be largely reduced when a suitable kinematic cut condition on $p_{J/\psi}$ and $\theta_{J/\psi}$ is implemented, where $p_{J/\psi}$ is the momentum of J/ψ and $\theta_{J/\psi}$ is the angle between J/ψ and the e^+e^- beam. In the range of $\pi/9 < \theta_{J/\psi} < 8\pi/9$ and $p_{J/\psi} > 3$ GeV, the cross section of the QED background is of the same order as that of the QCD contribution. Therefore, studying the J/ψ production with light hadrons is helpful to clarify the J/ψ production mechanism at B factories.

DOI: 10.1103/PhysRevD.100.114025

I. INTRODUCTION

The development of the nonrelativistic QCD (NRQCD) effective field theory [1] provides a powerful tool to study the production and decay of heavy quarkonium states that are constituted by one heavy quark (Q) and one heavy antiquark ($\bar{Q}$). The virtual difference between NRQCD factorization formalism and the conventional color-singlet model (CSM) is that NRQCD factorization includes the contribution of the $Q\bar{Q}$ state in the color-octet (CO) configuration, which is referred as the CO mechanism (COM). The role of COM has been extensively studied in various high energy experiments; for reviews, see Refs. [2–4]. Among them, the J/ψ production in e^+e^- annihilation at B factories (*BABAR* and Belle) has attracted considerable attention.

On the experimental side, the inclusive J/ψ production was measured by the *BABAR* [5] and Belle [6] collaborations in 2001. The Belle Collaboration further divided the inclusive J/ψ production rate into two pieces, $e^+e^- \to J/\psi + c\bar{c} + X$[1] and $e^+e^- \to J/\psi + X_{\text{non-c}\bar{\text{c}}}$ [8,9]. The latest results reported by the Belle Collaboration were [9]

$$\sigma(e^+e^- \to J/\psi + X) = 1.17 \pm 0.02 \pm 0.07 \text{ pb}, \tag{1a}$$

$$\sigma(e^+e^- \to J/\psi + c\bar{c} + X) = 0.74 \pm 0.08^{+0.09}_{-0.08} \text{ pb}, \tag{1b}$$

$$\sigma(e^+e^- \to J/\psi + X_{\text{non-c}\bar{\text{c}}}) = 0.43 \pm 0.09 \pm 0.09 \text{ pb}. \tag{1c}$$

For $J/\psi + c\bar{c} + X$ production, the CO contribution was found to be very small [10] and there were large discrepancies between Belle measurements and NRQCD predictions at leading order (LO) in α_s and v^2 [10–12], where v is the relative velocity between c and $\bar{c}$ in the meson rest frame. These puzzles were largely resolved after taking into account the next-to-leading order (NLO) QCD corrections [13,14] and relativistic corrections [15]. On the contrary, for $J/\psi + X_{\text{non-c}\bar{\text{c}}}$ production, the CO contribution from the $e^+e^- \to c\bar{c}({}^1S_0^{[8]}, {}^3P_J^{[8]}) + g$ process was found to be even

[1] The $J/\psi + c\bar{c} + X$ production includes both J/ψ in association with the charmed hadron pair and double charmonia production. The latter was also studied by the *BABAR* Collaboration [7].

larger than that of the CS $e^+e^- \to c\bar{c}(^3S_1^{[1]}) + gg$ process. At QCD LO, the cross sections of CO and CS processes were predicted to be about 0.3–0.8 pb [16–19] and 0.2–0.3 pb [11,20], respectively, depending on the choice of input parameters. Recently their NLO QCD corrections were calculated and the k-factors were found to be about 1.3 [21,22] and 1.9 [23] for the CS and CO processes, respectively. In addition, the relativistic corrections to the CS process were also obtained, which can enhance the LO result by a factor of about 1.2 [24,25]. Then up to the subleading order of α_s and v^2, the CS contribution itself can reach about 440–560 fb [24], which almost saturated the Belle measurement and left very little room for the CO contribution. Therefore, in the $e^+e^- \to J/\psi + X_{\text{non-}c\bar{c}}$ process, the conflict between NRQCD predictions and Belle's latest results is severe. By setting the CS contribution to zero, the upper bound of the CO long distance matrix elements (LDMEs) was obtained: $\langle 0|\mathcal{O}^{J/\psi}(^1S_0^{[8]})|0\rangle + 4.0\frac{\langle 0|\mathcal{O}^{J/\psi}(^3P_J^{[8]})|0\rangle}{m_c^2} < (2.0 \pm 0.6) \times 10^{-2}\ \text{GeV}^3$ [23]. When the CS contribution is properly included, the constraint becomes $\langle 0|\mathcal{O}^{J/\psi}(^1S_0^{[8]})|0\rangle + 4.0\frac{\langle 0|\mathcal{O}^{J/\psi}(^3P_J^{[8]})|0\rangle}{m_c^2} < 5.0 \times 10^{-3}\ \text{GeV}^3$ [4].

However, for J/ψ production in some other experiments, theoretical studies showed that the CO contribution is important. For example, (a) for J/ψ production from the Z-boson and Υ decays, there are still large gaps between CS predictions at QCD NLO and experimental measurements [26,27]; (b) for J/ψ photoproduction at HERA, the transverse momentum (p_t) distribution of J/ψ yields polarization parameters that can be reasonably well described after both the CS and CO contributions were included at QCD NLO [28–31]; (c) for J/ψ hadroproduction, despite the huge NLO QCD correction, the CS contribution is unable to account for the yield yet [32–34], and COM was found to play an important role [35–39], although the J/ψ polarization puzzle has not been resolved yet at QCD NLO [40–42]. By fitting to J/ψ hadroproduction data up to QCD NLO, different sets of CO LDMEs were obtained; however, all of their predictions for $J/\psi + X_{\text{non-}c\bar{c}}$ production at $\sqrt{s} = 10.6$ GeV overshoot Belle measurements [43]. Note that although the worldwide global fit result, which is calculated up to the order of $\alpha^2\alpha_s^2$, is compatible with Belle data [39,43], its prediction of J/ψ polarization at hadron colliders does not agree with data. Compared to the e^+e^- case, these studies gave an almost opposite conclusion about how large the CO contribution would be, or in other words, how large the values of the CO LDMEs could be.

To resolve the problem, we meticulously compare *BABAR*'s and Belle's measurements with theoretical calculation, and we find that there are some uncertainties which may potentially lead to a large influence on the current conclusion. A noticeable one is that the total cross section reported by the *BABAR* Collaboration [5] is about two times larger than that of Belle [9]. If we subtract the $J/\psi + c\bar{c} + X$ part, which was already well understood theoretically, from the *BABAR* measurement, there would be enough room left for the CO contribution. We find one possible reason for the disagreement between *BABAR* and Belle measurements is that they use different criteria to select data. In Belle's latest measurement [9], they only selected the event including at least five charge tracks in the final states and did not make up for it. This means that all events including zero or two charged light hadrons, for example, $J/\psi + m(\pi^+\pi^-) + n\pi^0$ for ($m = 0, 1$; $n = 0, 1, 2\ldots$), were all excluded. From the point view of quark-hadron duality, Belle's measurement is only a part of NRQCD prediction. To reduce the uncertainty mentioned above and understand the J/ψ production mechanism in e^+e^- annihilation, we suggest measuring the complete cross section for the $J/\psi + X_{\text{non-}c\bar{c}}$ process by including the events with a number of charged tracks less than five in the final state as well, which is equivalent to measuring the complete cross section of J/ψ production with light hadrons. To avoid potential unnecessary confusion with Belle's notation, we now call the complete process of J/ψ production without the association of a charm quark pair as $J/\psi + X_{\text{non-}c\bar{c}}^{N_{ch}\geq 0}$. Thus, the NRQCD predictions can be compared with experimental measurements directly.

One big obstacle preventing us from measuring $J/\psi + X_{\text{non-}c\bar{c}}^{N_{ch}\geq 0}$ production is the large QED background due to $\psi(2S) \to J/\psi + \pi\pi$,[2] where $\psi(2S)$ is produced through the initial state radiation (ISR) process $e^+e^- \to \psi(2S) + \gamma$, higher order QED processes $e^+e^- \to \psi(2S) + f\bar{f}$ (f can be lepton or light quark), and due to direct J/ψ production through $e^+e^- \to J/\psi + q\bar{q}$ process with the $q = u, d, s$ quark. The branching function for τ hadronic decay is very large; however, the total cross section of $e^+e^- \to J/\psi + \tau\bar{\tau}$ is so small that it can be ignored. To help remove them from the experimental measurements, in this work, we will present a detailed study on $\psi(2S)$ and $J/\psi + q\bar{q}$ production in such QED processes and discuss its influence on $J/\psi + X_{\text{non-}c\bar{c}}^{N_{ch}\geq 0}$ measurement.

II. FRAMEWORK OF CALCULATION

For $J/\psi + \pi\pi$ production from $\psi(2S)$ feed-down, the Feynman amplitude $\mathcal{M}$ can be generally expressed as

$$\mathcal{M} = \mathcal{M}_\mu^{\psi(2S)}(P_{2S}) \times \frac{-g^{\mu\nu} + \frac{P_{2S}^\mu P_{2S}^\nu}{P_{2S}^2}}{P_{2S}^2 - M_{2S}^2 + i * M_{2S}\Gamma} \mathcal{M}_\nu^{(\psi(2S)\to J/\psi+\pi\pi)}$$
$$= \frac{\mathcal{M}_0}{P_{2S}^2 - M_{2S}^2 + i * M_{2S}\Gamma}, \tag{2}$$

[2] $\psi(2S)$ can also decay into $J/\psi + \eta$. However, the branching ratio is about 15 times less than the 2π channel, so we can drop it safely in our calculation.

where $\mathcal{M}_\mu^{\psi(2S)}(P_{2S})$ is the amplitude for $\psi(2S)$ production with momentum P_{2S}, $\mathcal{M}_\nu^{(\psi(2S)\to J/\psi+\pi\pi)}$ is the amplitude for $\psi(2S)$ decay into $J/\psi+\pi\pi$, and Γ is the total decay width of $\psi(2S)$. In the narrow-width approximation, the absolute square of the $\psi(2S)$ propagator becomes

$$\lim_{\Gamma\to 0}\frac{1}{(P_{2S}^2-M_{2S}^2)^2+M_{2S}^2\Gamma^2}=\frac{\pi\delta(P_{2S}^2-M_{2S}^2)}{M_{2S}\Gamma}. \quad (3)$$

Combining with the complete phase space integration, we obtain

$$\sigma=\frac{1}{8s}\times\frac{1}{2M_{2S}\Gamma}\int d\mathrm{LIPS}_1\int d\mathrm{LIPS}_2\sum|\mathcal{M}_0|^2, \quad (4)$$

where LIPS_1 is the phase space of $\psi(2S)$ production, LIPS_2 is the phase space of $\psi(2S)$ decay into $J/\psi+\pi\pi$, and $\sum$ means the sum over the spin of initial and final states. If we are only interested in the total but not differential cross section, $|M_0|^2$ can be further factorized as

$$\sum|M_0|^2=\frac{1}{2J+1}\sum|\mathcal{M}^{\psi(2S)}|^2\times\sum|\mathcal{M}^{(\psi(2S)\to J/\psi+\pi\pi)}|^2 \quad (5)$$

with $J=1$ the spin of $\psi(2S)$. We would like to remind the reader that the factorization formula can only be applied to the total cross section for $\psi(2S)$ feed-down to J/ψ via $\psi(2S)\to J/\psi+\pi\pi$. For the differential or cross section under some cut conditions, only the complete formula Eq. (4) works, where the correlation effect between $\psi(2S)$ and J/ψ is included.

We use the effective Lagrangian method to describe $\psi(2S)\to J/\psi+\pi\pi$. The amplitude $\mathcal{M}^{(\psi(2S)\to J/\psi+\pi\pi)}$ can be read directly as [44]

$$\begin{aligned}&\mathcal{M}^{(\psi(2S)\to J/\psi+\pi(p_1)\pi(p_2))}\\&=-\frac{4}{F_0^2}\left[\left(\frac{g}{2}(m_{\pi\pi}^2-2M_\pi^2)+g_1(v\cdot p_1)(v\cdot p_2)+g_3M_\pi^2\right)\right.\\&\quad\left.\times\epsilon_{J/\psi}^*\cdot\epsilon_{\psi(2S)}+g_2(p_{1\mu}p_{2\nu}+p_{1\nu}p_{2\mu})\epsilon_{J/\psi}^{*\mu}\epsilon_{\psi(2S)}^\nu\right],\end{aligned} \quad (6)$$

where $m_{\pi\pi}^2=(p_1+p_2)^2$, M_π is the mass of the π meson, $v=(1,\vec{0})$ in the $\psi(2S)$ rest frame, and $F_0\simeq 93$ MeV [44]. The coupling constant $g_2\simeq 0$, because it is strongly suppressed by the chiral symmetry breaking scale over m_c. By fitting the data of $\psi(2S)\to J/\psi+\pi^+\pi^-$, the BES Collaboration obtained two sets of values for $\frac{g_1}{g}$ and $\frac{g_3}{g}$ [45]. Together with $\mathrm{Br}(\psi(2S)\to J/\psi+\pi^+\pi^-)=33.6\%$ [46], we get[3]

$$g=0.322,\qquad \frac{g_1}{g}=-0.49,\qquad \frac{g_3}{g}=0.54, \quad (7)$$

or

$$g=0.319,\qquad \frac{g_1}{g}=-0.347,\qquad g_3=0. \quad (8)$$

In NRQCD factorization, the Feynman amplitude $\mathcal{M}^{\psi(2S)}$ for $e^+e^-\to\psi(2S)+X$ can be expressed as

$$\begin{aligned}\mathcal{M}^{\psi(2S)}=&\sqrt{C_{2S}}\sum_{s_1,s_2}\sum_{i,j}\langle s_1;s_2|1S_z\rangle\langle 3i;\bar{3}j|1\rangle\\&\times\mathcal{A}\left(e^+e^-\to c_i\left(\frac{P_{2S}}{2},s_1\right)\right.\\&\left.+\bar{c}_j\left(\frac{P_{2S}}{2},s_2\right)+X\right),\end{aligned} \quad (9)$$

where $\mathcal{A}$ is the standard Feynman amplitude for $e^+e^-\to c_i(\frac{P_{2S}}{2},s_1)+\bar{c}_j(\frac{P_{2S}}{2},s_2)+X$, and $\langle s_1;s_2|1S_z\rangle$ and $\langle 3i;\bar{3}j|1\rangle=1/\sqrt{N_c}$ are the SU(2)-spin and SU(3)-color Clebsch-Gordan coefficients for $c\bar{c}$ projecting on the spin-triplet CS S-wave state. The projection of Dirac spinors can be rewritten as

$$\begin{aligned}&\sum_{s_1,s_2}\langle s_1;s_2|1S_z\rangle v\left(\frac{P_{2S}}{2},s_2\right)\bar{u}\left(\frac{P_{2S}}{2},s_1\right)\\&=\frac{1}{2\sqrt{2}}\not\epsilon^*(S_z)(\not P_{2S}+M_{2S}).\end{aligned} \quad (10)$$

C_{2S} is the LDME that can be related to $\psi(2S)$ wave function at the origin through $C_{2S}=\frac{1}{4\pi}|R_{2S}(0)|^2$ or can be determined from the leptonic decay of $\psi(2S)$ via

$$\Gamma(\psi(2S)\to e^+e^-)=\frac{256\pi^2\alpha^2C_{2S}}{9M_{2S}^2}. \quad (11)$$

In this work, we choose the value determined from Eq. (11).

III. THE FEED-DOWN BACKGROUND FROM $e^+e^-\to\psi(2S)+\gamma$

The typical Feynman diagram for the ISR process $e^+e^-\to\psi(2S)+\gamma$ followed by $\psi(2S)\to J/\psi+\pi\pi$ is shown in Fig. 1(a). Using the formula introduced in Eqs. (10)–(11), $|\mathcal{M}_0^2|$ and $|\mathcal{M}(e^+e^-\to\psi(2S)+\gamma)|^2$ can be computed straightforwardly. The analytical expression of $|\mathcal{M}_0^2|$ is lengthy. We will not present it here but only $|\mathcal{M}(e^+e^-\to\psi(2S)+\gamma)|^2$:

[3]These parameters can also well reproduce the decay width of $\psi(2S)\to J/\psi+\pi^0\pi^0$.

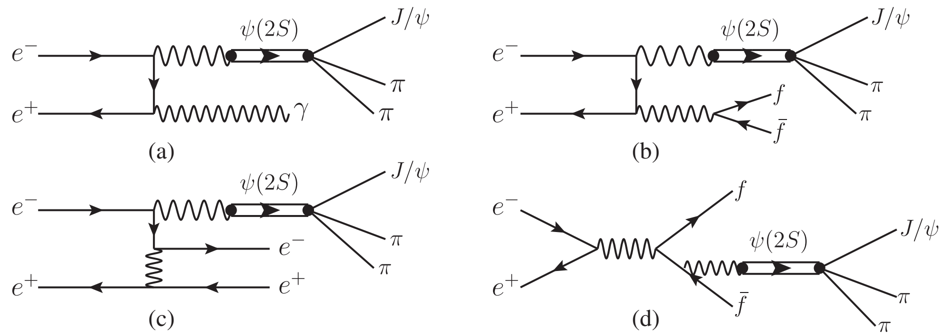

FIG. 1. The typical diagrams describing the $\psi(2S)$ feed-down background.

$$
\begin{aligned}
&|\mathcal{M}(e^+e^- \to \psi(2S)+\gamma)|^2 \\
&\quad = \frac{96 e_c^2 (4\pi\alpha)^3 C_{2S}}{sr(-1+r+(-1+r)(-1+4r_e)x_2^2)^2}(-1-2r-r^2 \\
&\qquad - 8r_e + 16 r r_e + 32 r_e^2 - 4(r+2r_e)(-1+4r_e)x_2^2 \\
&\qquad + (-1+r)^2(1-4r_e)^2 x_2^4),
\end{aligned} \tag{12}
$$

where $e_c = \frac{2}{3}$, $r = \frac{M_{2S}^2}{s}$, $r_e = \frac{M_e^2}{s}$, and $x_2 = \cos(\theta_{\psi(2S)})$, with $\theta_{\psi(2S)}$ the angle between $\psi(2S)$ and the e^+e^- beam. In the limit of $r_e = 0$, Eq. (12) has a simple form:

$$
\begin{aligned}
&|\mathcal{M}(e^+e^- \to \psi(2S)+\gamma)|^2 \\
&\quad = \frac{96 e_c^2 (4\pi\alpha)^3 C_{2S}}{s}\left(\frac{1}{r} - \frac{2(1+r^2)}{r(1-r)^2(1-x_2^2)}\right).
\end{aligned} \tag{13}
$$

Choosing $M_{2S} = 3.686$ GeV, $m_e = 0.51$ MeV, $\alpha = \frac{1}{137}$, and $\Gamma(\psi(2S) \to e^+e^-) = 4.30$ keV [46], we get

$$\sigma(e^+e^- \to \psi(2S)+\gamma) = 13.22 \text{ pb}, \tag{14}$$

and the feed-down cross section is

$$
\begin{aligned}
&\sigma(e^+e^- \to \psi(2S)+\gamma) \times \mathrm{Br}(\psi(2S) \to J/\psi + \pi\pi) \\
&\quad = 6.79 \text{ pb},
\end{aligned} \tag{15}
$$

which, as expected, is very large. The reason is that in the limit of $m_e \to 0$, Eq. (13) is divergent at $x_2 = \pm 1$. The angular distribution $d\sigma(e^+e^- \to \psi(2S)+\gamma)/dx_2$ is given in Fig. 2. It clearly shows that the differential cross section drops down very fast when the direction of $\psi(2S)$ deviates a little from the beam line. If we impose a cut on x_2, i.e., the angle $\theta_{\psi(2S)}$, the cross section is largely shrunk. In different cut conditions, the results are

$$\sigma(e^+e^- \to \psi(2S)+\gamma) \times \mathrm{Br}(\psi(2S) \to J/\psi + \pi\pi)|_{\frac{\pi}{18} < \theta_{\psi(2S)} < \frac{17\pi}{18}} = 1.48 \text{ pb}, \tag{16a}$$

$$\sigma(e^+e^- \to \psi(2S)+\gamma) \times \mathrm{Br}(\psi(2S) \to J/\psi + \pi\pi)|_{\frac{\pi}{9} < \theta_{\psi(2S)} < \frac{8\pi}{9}} = 0.99 \text{ pb}, \tag{16b}$$

$$\sigma(e^+e^- \to \psi(2S)+\gamma) \times \mathrm{Br}(\psi(2S) \to J/\psi + \pi\pi)|_{\frac{\pi}{6} < \theta_{\psi(2S)} < \frac{5\pi}{6}} = 0.71 \text{ pb}. \tag{16c}$$

Let $p_{J/\psi}^{*\mu}$ denote the four-momentum of J/ψ in the rest frame of $\psi(2S)$. Thus the range of the J/ψ velocity, $|v^*| = |\vec{\mathbf{p}}_{J/\psi}^*|/E_{J/\psi}^*$, is from 0 to 0.15. It is much smaller than the velocity of $\psi(2S)$ in the e^+e^- center of mass frame (CMF), which is about 0.78. Therefore, normally the direction of J/ψ in the e^+e^- CMF can be treated approximately as that of $\psi(2S)$. Such an approximation may not work well here since the cross section in Eq. (15) is 1 order of magnitude larger than the QCD contribution from the CS process [24]. A slight difference may lead to an unavoidable effect. Therefore, we also calculate the cross section rigorously with Eq. (4). Let $\theta_{J/\psi}$ be the angle between J/ψ and the e^+e^- beam in the e^+e^- CMF. Then $x_2' = \cos(\theta_{J/\psi})$ can be expressed as

$$x_2' = \frac{\mathbf{k}_1 \cdot \mathbf{p}_{J/\psi}'}{|\mathbf{k}_1||\mathbf{p}_{J/\psi}'|}, \qquad p_{J/\psi}'^{\mu} = L_\nu^\mu p_{J/\psi}^{*\nu}, \tag{17}$$

where k_1^μ is the e^+ four-momentum, L_ν^μ is the Lorentz matrix that boosts $p_{J/\psi}^{*\nu}$ from the $\psi(2s)$ rest frame to the e^+e^- CMF. We perform the numerical computation by using the Feynman Diagram Calculation (FDC) package [47] with the inputs of pion masses as $M_{\pi^+} = M_{\pi^-} = 140$ MeV and

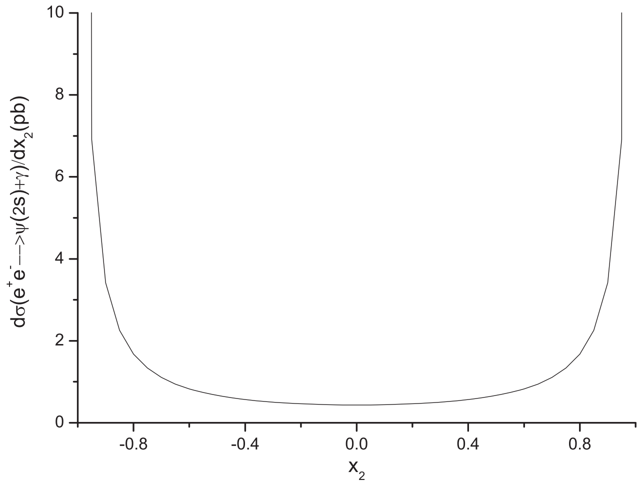

FIG. 2. The angular distribution of $\psi(2S)$ in the ISR process $e^+e^- \to \psi(2S) + \gamma$, where $x_2 = \cos(\theta_{\psi(2S)})$ and $\theta_{\psi(2S)}$ is the angle between $\psi(2S)$ and the e^+e^- beam.

$M_{\pi^0} = 135$ MeV. When we choose the first set of values in Eq. (7) for g, g_1 and g_3, the cross section in different cut conditions becomes

$$\sigma(e^+e^- \to (J/\psi + \pi\pi)_{\psi(2S)} + \gamma)|_{\frac{\pi}{18}<\theta_{J/\psi}<\frac{17\pi}{18}} = 1.51 \text{ pb}; \tag{18a}$$

$$\sigma(e^+e^- \to (J/\psi + \pi\pi)_{\psi(2S)} + \gamma)|_{\frac{\pi}{9}<\theta_{J/\psi}<\frac{8\pi}{9}} = 0.99 \text{ pb}; \tag{18b}$$

$$\sigma(e^+e^- \to (J/\psi + \pi\pi)_{\psi(2S)} + \gamma)|_{\frac{\pi}{6}<\theta_{J/\psi}<\frac{5\pi}{6}} = 0.71 \text{ pb}. \tag{18c}$$

Alternatively, if we choose the values in Eq. (8), the corresponding cross sections become

$$\sigma(e^+e^- \to (J/\psi + \pi\pi)_{\psi(2S)} + \gamma)|_{\frac{\pi}{18}<\theta_{J/\psi}<\frac{17\pi}{18}} = 1.52 \text{ pb}; \tag{19a}$$

$$\sigma(e^+e^- \to (J/\psi + \pi\pi)_{\psi(2S)} + \gamma)|_{\frac{\pi}{9}<\theta_{J/\psi}<\frac{8\pi}{9}} = 1.00 \text{ pb}; \tag{19b}$$

$$\sigma(e^+e^- \to (J/\psi + \pi\pi)_{\psi(2S)} + \gamma)|_{\frac{\pi}{6}<\theta_{J/\psi}<\frac{5\pi}{6}} = 0.71 \text{ pb}. \tag{19c}$$

The numerical results in Eqs. (16), (18), and (19) show that for the J/ψ production from $\psi(2S)$ feed-down in the ISR process at $\sqrt{s} = 10.6$ GeV, the approximation

$$\frac{d\sigma(e^+e^- \to (J/\psi + \pi\pi)_{\psi(2S)} + \gamma)}{d\cos(\theta_{J/\psi})} = \frac{d\sigma(e^+e^- \to \psi(2S) + \gamma) \times \mathrm{Br}(\psi(2S) \to J/\psi + \pi\pi)}{d\cos(\theta_{\psi(2S)})} \tag{20}$$

holds well in the range of $\pi/18 < \theta_{J/\psi} < 17\pi/18$, and the difference between exact and approximate calculation is within 5% and a few fb for the cross section. A deeper reason is that the J/ψ in the decay subprocess is almost static in the $\psi(2S)$ rest frame as can be figured out from the $\pi\pi$ invariant mass spectrum [45]. Furthermore, the J/ψ angular distribution is almost independent of the details of $\psi(2S)$ decay.

The energy difference between $\psi(2S)$ and J/ψ is of $m_c v^2$ order. According to the power counting in NRQCD factorization, it is of the same order as the soft gluon energy emitted by the CO ${}^3P_J^{[8]}$ or ${}^1S_0^{[8]}$ state during their evolution into J/ψ [1]. Thus, the momentum carried by J/ψ from the ISR $\psi(2s)$ feed-down would be very similar to that of J/ψ produced via the CO channel in the LO QCD calculation, which is close to the kinematic end point. It was also shown that after including the NLO QCD corrections, the predominant CO contribution still assembles near the kinematic end point region [23]. To help separate the possible CO signal from the ISR QED background $e^+e^- \to \psi(2S) + \gamma$, it is good to know the J/ψ momentum distribution in the feed-down background as well. We compute it numerically for different $\theta_{J/\psi}$ cuts using the two sets of parameters in Eqs. (7) and (8) too. The results are shown in Figs. 3(a)–3(d). We observe from these plots that, similar to the angular distribution case, the J/ψ momentum spectra in the ISR $\psi(2S)$ feed-down background are not sensitive to the two sets of parameters in Eqs. (7) and (8) either. Hence for simplicity, the following results are all calculated with inputs for g, g_1, and g_3 from Eq. (7).

IV. BACKGROUND FROM HIGHER QED PROCESSES

In direct J/ψ production, the cross section of the higher order QED process $e^+e^- \to J/\psi + f + \bar{f}$ is considerable [48], where f can be the lepton or light quark, so the $e^+e^- \to \psi(2S) + f + \bar{f}$ may also be an important source of the $J/\psi + X_{\text{non-}c\bar{c}}^{N_{ch}\geq 0}$ background. The typical Feynman diagrams for $f \neq e$ are shown in Figs. 1(b) and 1(d). For $f = e$, there is an additional t-channel contribution, the typical Feynman diagram of which is shown in Fig. 1(c). Because of the t-channel enhancement, the cross section for $f = e$ is expected to be much larger than that for $f \neq e$. In the subsections, we will discuss $f = e$ and $f \neq e$ separately. At this order, in addition to $\psi(2S)$ feed-down, there is also a sizable QED contribution

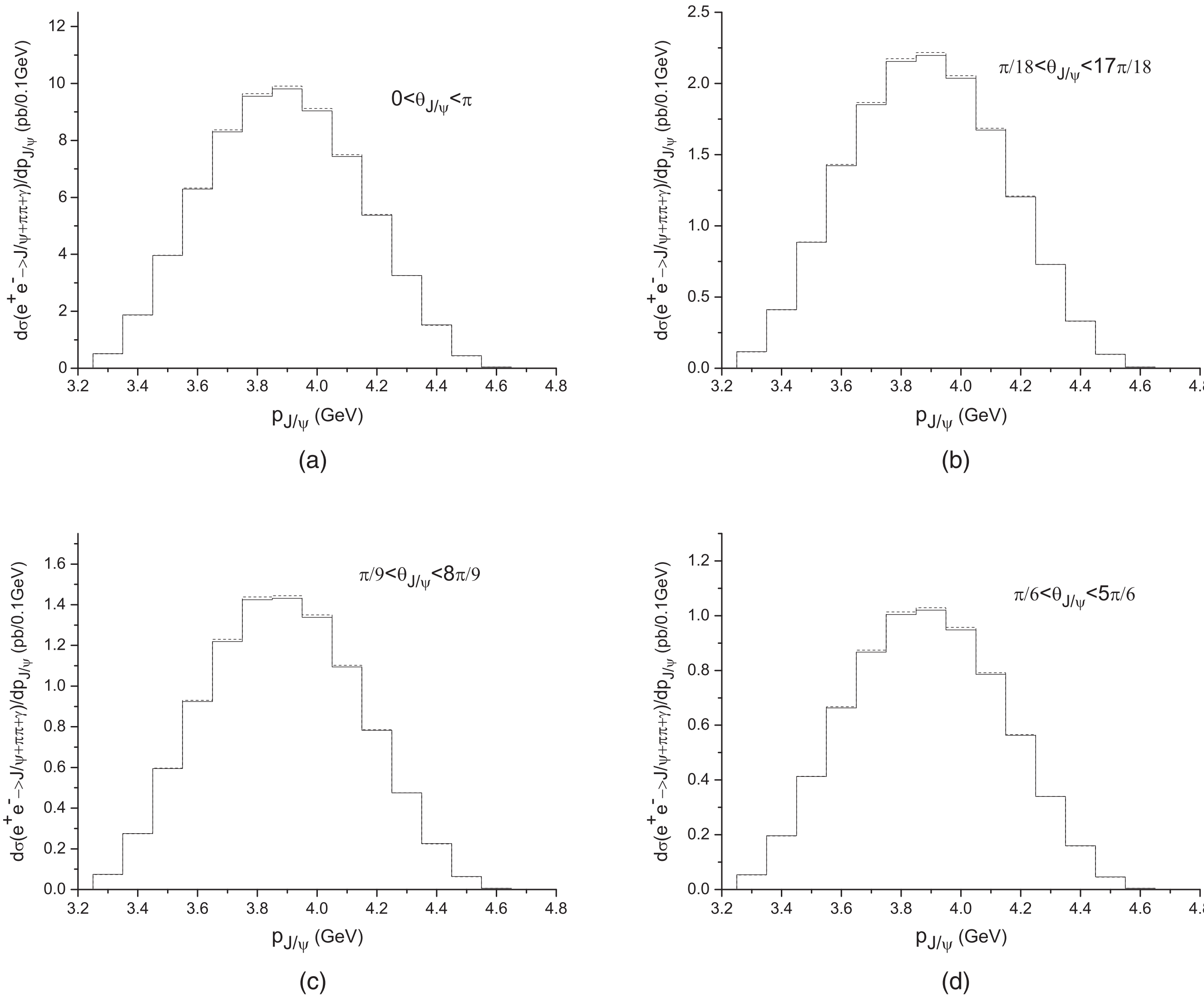

FIG. 3. The momentum spectra of J/ψ produced from the feed-down of the ISR $\psi(2S)$ process in different cut conditions of $\theta_{J/\psi}$ by using two different sets of parameters in Eq. (7) (solid line) and Eq. (8) (dashed line) to describe $\psi(2S) \to J/\psi + \pi\pi$.

from direct $J/\psi + q\bar{q}$ production with the $q = u,\ d,\ s$ quark. We will also discuss it in Sec. IV C.

A. The feed-down background from $e^+e^- \to \psi(2S) + e^+e^-$

According to the topology of Feynman diagrams for $e^+e^- \to \psi(2S) + e^+e^-$, we divide the process into three parts: the t-channel part [Fig. 1(c)], the two-photon channel part [Fig. 1(b)], and the s-channel part [Fig. 1(d)]. It is easy to check that the Feynman amplitude for each part itself is gauge invariant. Compared to the cross section $\sigma^{\rm T}$ of the t-channel part, the cross sections of the two-photon part $\sigma^{\rm TP}$ and the s-channel part $\sigma^{\rm S}$ are suppressed by the factors $\frac{M^2_{\psi(2S)}}{s}$ and $\frac{M^2_{\psi(2S)}}{s}\ln^{-2}(\frac{s}{4M_e^2})$, respectively, which are about 10^{-1} and 10^{-4} at $\sqrt{s} = 10.6$ GeV. Choosing the same values for the parameters as in the ISR process, we obtain

$$\sigma^{\rm T}(e^+e^- \to (J/\psi + \pi\pi)_{\psi(2S)} + e^+e^-) = 0.50\ \text{pb}; \quad (21a)$$

$$\sigma^{\rm TP}(e^+e^- \to (J/\psi + \pi\pi)_{\psi(2S)} + e^+e^-) = 4.8 \times 10^{-2}\ \text{pb}; \quad (21b)$$

$$\sigma^{\rm S}(e^+e^- \to (J/\psi + \pi\pi)_{\psi(2S)} + e^+e^-) = 8.5 \times 10^{-4}\ \text{pb}, \quad (21c)$$

which is consistent with the qualitative estimation. The cross section of the s-channel part is only about 1 fb. It is so small that we drop it in further analysis. The angular

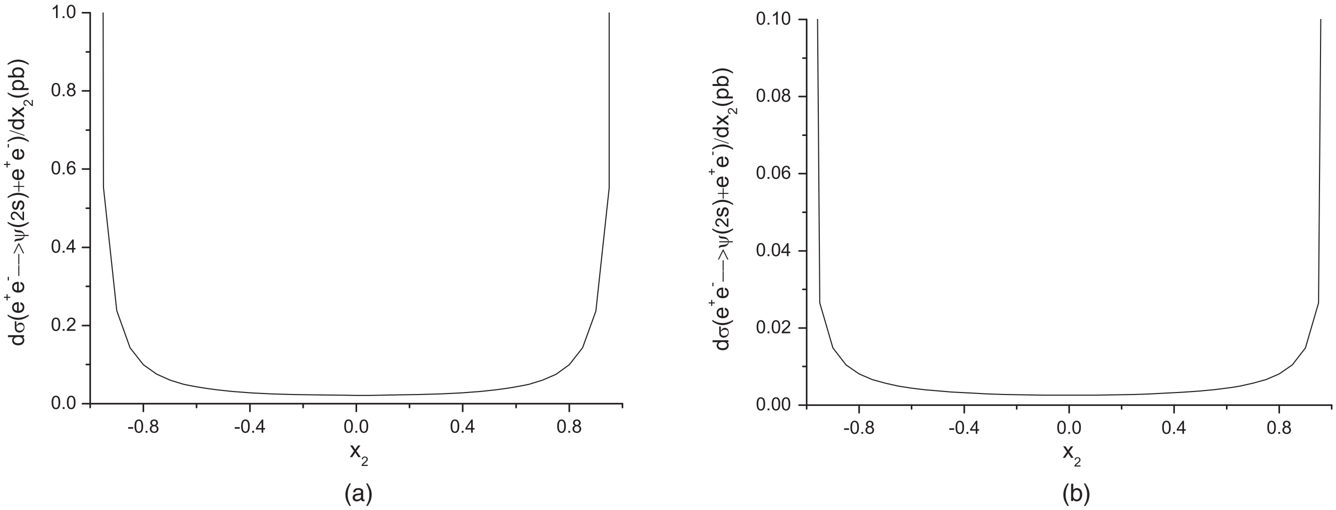

FIG. 4. The angular distribution of $\psi(2S)$ produced through (a) the t-channel and (b) two-photon channel in the $e^+e^- \to \psi(2S) + e^+e^-$ process, where $x_2 = \cos(\theta_{\psi(2S)})$, and $\theta_{\psi(2S)}$ is the angle between $\psi(2S)$ and the e^+e^- beam.

distributions of $\psi(2S)$ in the t-channel and two-photon channel are shown in Fig. 4. Unlike the ISR process, the momentum of J/ψ from feed-down via $e^+e^- \to \psi(2S) + e^+e^-$ ranges from 0 to 4.7 GeV. We also calculate the momentum spectra for the t-channel and two-photon channel parts. The results are shown in Fig. 5.

If we set the same cut on $\theta_{J/\psi}$, σ^{T} and σ^{TP} both drop down largely too:

$$\sigma^{\mathrm{T(TP)}}(e^+e^- \to (J/\psi + \pi\pi)_{\psi(2S)} + e^+e^-)|_{\frac{\pi}{18}<\theta_{J/\psi}<\frac{17\pi}{18}} = 0.105(0.019)\ \mathrm{pb}; \tag{22a}$$

$$\sigma^{\mathrm{T(TP)}}(e^+e^- \to (J/\psi + \pi\pi)_{\psi(2S)} + e^+e^-)|_{\frac{\pi}{9}<\theta_{J/\psi}<\frac{8\pi}{9}} = 0.059(0.013)\ \mathrm{pb}; \tag{22b}$$

$$\sigma^{\mathrm{T(TP)}}(e^+e^- \to (J/\psi + \pi\pi)_{\psi(2S)} + e^+e^-)|_{\frac{\pi}{6}<\theta_{J/\psi}<\frac{5\pi}{6}} = 0.039(0.010)\ \mathrm{pb}. \tag{22c}$$

We also study the interference effect between the t-channel and two-photon channel and find it is very small. The cross section of the interference part is about -20 fb in the whole phase space region. The angular distribution of the $\psi(2S)$ and J/ψ momentum spectrum without a kinematic cut can be obtained approximately by adding the contributions from the t-channel and two-photon channel since the interference effect is very small. After including the interference part, the total cross section with different cuts for $\theta(J/\psi)$ becomes

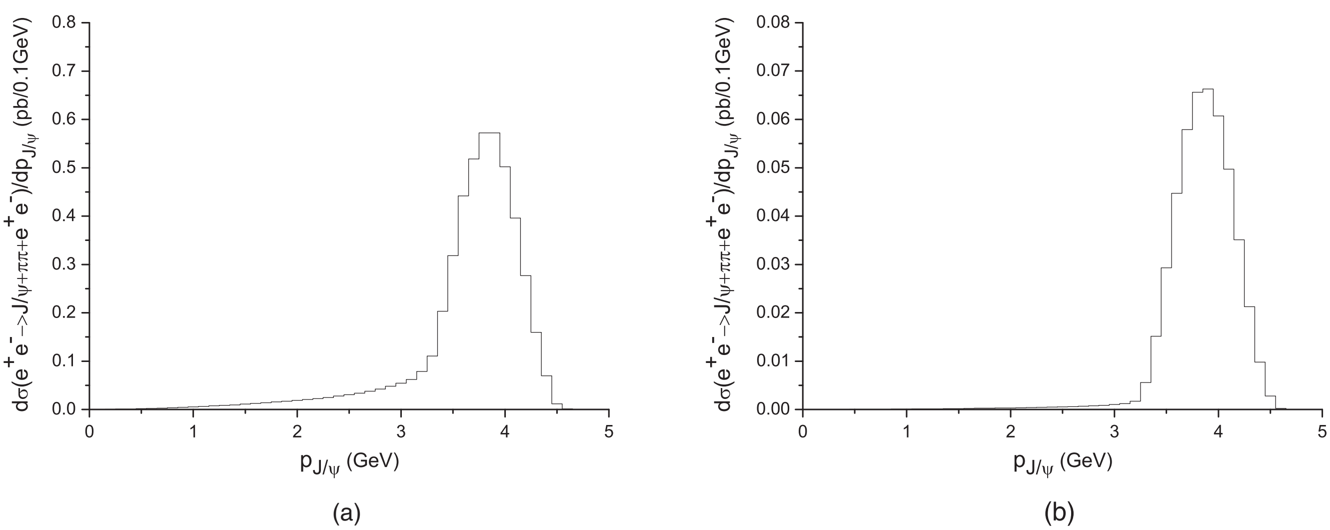

FIG. 5. The momentum distribution of J/ψ produced through (a) the t-channel and (b) two-photon channel in the $e^+e^- \to \psi(2S) + e^+e^-$ process.

$$\sigma(e^+e^- \to (J/\psi+\pi\pi)_{\psi(2S)} + e^+e^-)|_{\frac{\pi}{18}<\theta_{J/\psi}<\frac{17\pi}{18}} = 0.12 \text{ pb}; \tag{23a}$$

$$\sigma(e^+e^- \to (J/\psi+\pi\pi)_{\psi(2S)} + e^+e^-)|_{\frac{\pi}{9}<\theta_{J/\psi}<\frac{8\pi}{9}} = 0.070 \text{ pb}; \tag{23b}$$

$$\sigma(e^+e^- \to (J/\psi+\pi\pi)_{\psi(2S)} + e^+e^-)|_{\frac{\pi}{6}<\theta_{J/\psi}<\frac{5\pi}{6}} = 0.047 \text{ pb}. \tag{23c}$$

B. The feed-down background from $e^+e^- \to \psi(2S) + f\bar{f}(f \neq e)$

The process $e^+e^- \to \psi(2S) + f\bar{f}(f \neq e)$ has been fully studied in Ref. [49]. For completeness, we also compute it independently and obtain

$$\sum_{f=\mu,\tau,u,d,s} \sigma(e^+e^- \to (J/\psi+\pi\pi)_{\psi(2S)} + f\bar{f}) = 0.026 \text{ pb}. \tag{24}$$

If we set the same cut on $\theta_{J/\psi}$ as we do in the above, the cross sections become

$$\sum_{f=\mu,\tau,u,d,s} \sigma(e^+e^- \to (J/\psi+\pi\pi)_{\psi(2S)} + f\bar{f})|_{\frac{\pi}{18}<\theta_{J/\psi}<\frac{17\pi}{18}} = 0.020 \text{ pb}; \tag{25a}$$

$$\sum_{f=\mu,\tau,u,d,s} \sigma(e^+e^- \to (J/\psi+\pi\pi)_{\psi(2S)} + f\bar{f})|_{\frac{\pi}{9}<\theta_{J/\psi}<\frac{8\pi}{9}} = 0.015 \text{ pb}; \tag{25b}$$

$$\sum_{f=\mu,\tau,u,d,s} \sigma(e^+e^- \to (J/\psi+\pi\pi)_{\psi(2S)} + f\bar{f})|_{\frac{\pi}{6}<\theta_{J/\psi}<\frac{5\pi}{6}} = 0.011 \text{ pb}. \tag{25c}$$

The cross sections in different cut regions are about 0.010–0.020 pb. Since they are about $4 \simeq 6$ times less than those in the $e^+e^- \to \psi(2S) + e^+e^-$ process, we will not present further analysis here and recommend Ref. [49] for more detailed discussion.

C. The background from $e^+e^- \to J/\psi + q\bar{q}$

The Feynman diagrams for the $e^+e^- \to J/\psi + q\bar{q}$ process are similar to those for the $e^+e^- \to \psi(2S) + q\bar{q}$ process. In $\psi(2S)$ production, the contribution of the s-channel part can be ignored; thus we will not include it here. The cross section of $e^+e^- \to J/\psi + q\bar{q}$ has also been calculated in Ref. [49], which is not small. Using the method introduced in Ref. [49], we calculate the cross section with different constraints on $\theta_{J/\psi}$ and get

$$\sum_{q=u,d,s} \sigma(e^+e^- \to J/\psi + q\bar{q})|_{\frac{\pi}{18}<\theta_{J/\psi}<\frac{17\pi}{18}} = 0.071 \text{ pb}; \tag{26a}$$

$$\sum_{q=u,d,s} \sigma(e^+e^- \to J/\psi + q\bar{q})|_{\frac{\pi}{9}<\theta_{J/\psi}<\frac{8\pi}{9}} = 0.052 \text{ pb}; \tag{26b}$$

$$\sum_{q=u,d,s} \sigma(e^+e^- \to J/\psi + q\bar{q})|_{\frac{\pi}{6}<\theta_{J/\psi}<\frac{5\pi}{6}} = 0.039 \text{ pb}. \tag{26c}$$

The J/ψ angular and momentum distributions are shown in Fig. 6. The difference between our results and those in Ref. [49] is due to the different choices of the parameters and amount of data samples used in the R-value curve [46]. The branching function of τ leptons to light hadrons is more

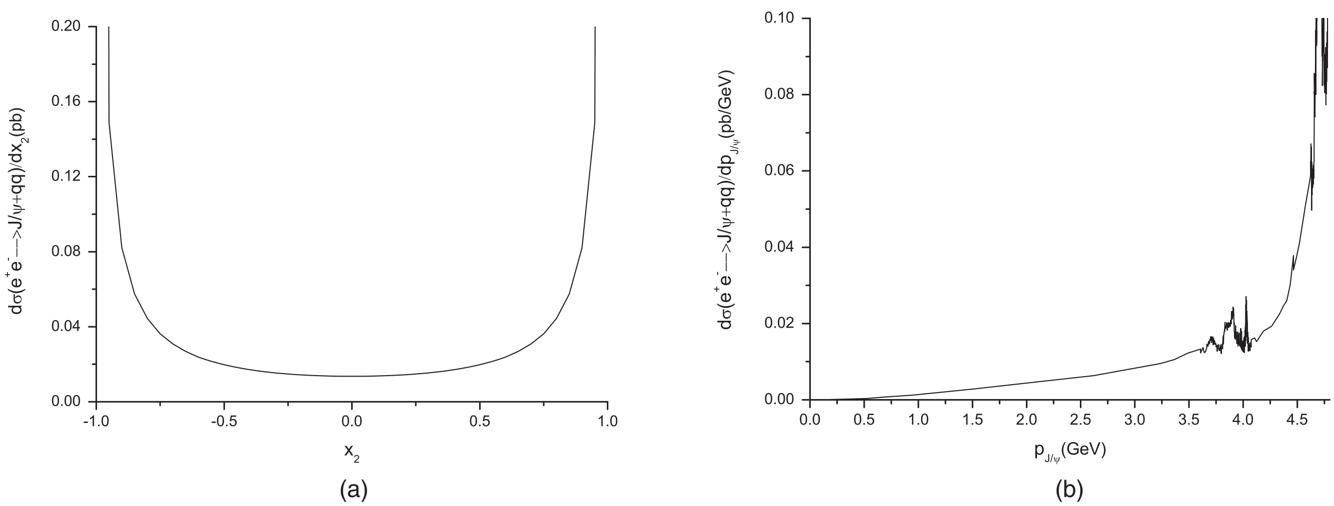

FIG. 6. The angular (a) and momentum (b) distributions of J/ψ in the process of $e^+e^- \to J/\psi + q\bar{q}$, where $x_2' = \cos(\theta_{J/\psi})$, and $\theta_{J/\psi}$ is the angle between $\theta_{J/\psi}$ and the e^+e^- beam.

than 60%, yet the total cross section of $e^+e^- \to J/\psi + \tau\bar{\tau}$ is only a few fb [49]. We, therefore, do not include them.

V. CONCLUSIONS AND DISCUSSIONS

Summing up all the contributions from the ISR and $f\bar{f}$ processes due to $\psi(2S)$ feed-down and that from the direct $J/\psi + q\bar{q}$ process, the total cross section of QED background is about

$$\sigma_{\mathrm{QED}}(e^+e^- \to J/\psi + X_{\text{non-}c\bar{c}}^{N_{ch}\geq 0}) = 7.46 \text{ pb}, \tag{27}$$

which is more than 1 order of magnitude larger than that of the conventional QCD processes $e^+e^- \to J/\psi + X_{\text{non-}c\bar{c}}^{N_{ch}\geq 0}$ [11,21–23]. Such a huge background makes it difficult to measure the interesting QCD contribution in the whole phase space region. We found that the background will drop down deeply if we set a cut on $\theta_{J/\psi}$, for example,

$$\sigma_{\mathrm{QED}}(e^+e^- \to J/\psi + X_{\text{non-}c\bar{c}}^{N_{ch}\geq 0})|_{\frac{\pi}{18}<\theta_{J/\psi}<\frac{17\pi}{18}} = 1.73 \text{ pb}; \tag{28a}$$

$$\sigma_{\mathrm{QED}}(e^+e^- \to J/\psi + X_{\text{non-}c\bar{c}}^{N_{ch}\geq 0})|_{\frac{\pi}{9}<\theta_{J/\psi}<\frac{8\pi}{9}} = 1.14 \text{ pb}; \tag{28b}$$

$$\sigma_{\mathrm{QED}}(e^+e^- \to J/\psi + X_{\text{non-}c\bar{c}}^{N_{ch}\geq 0})|_{\frac{\pi}{6}<\theta_{J/\psi}<\frac{5\pi}{6}} = 0.81 \text{ pb}. \tag{28c}$$

In NRQCD factorization, the conventional $J/\psi + X_{\text{non-}c\bar{c}}^{N_{ch}\geq 0}$ production includes both the CS and CO contributions. For the CS $e^+e^- \to J/\psi + gg$ process, both the NLO QCD [21] and relativistic corrections [24,25] have been calculated. The cross section at NLO in α_s and v_c^2 is about 0.4–0.7 pb [21,22,24]. The NLO QCD corrections to the CO contribution have also been obtained [23]. If we choose $\langle 0|\mathcal{O}^{J/\psi}(^1S_0^{[8]})|0\rangle = (3.04 \pm 0.35) \times 10^{-2}$ GeV^3, $\langle 0|\mathcal{O}^{J/\psi}(^3P_J^{[8]})|0\rangle = (-9.08 \pm 1.61) \times 10^{-3}$ GeV^5, which were obtained by a global fit to J/ψ worldwide data [39], the cross section of the CO contribution at QCD NLO will be about 0.3 pb for $\mu = 2m_c$, $\alpha_s(\mu) = 0.245$. Thus in total, NRQCD prediction for σ_{QCD} of the conventional $J/\psi + X_{\text{non-}c\bar{c}}^{N_{ch}\geq 0}$ production will be about 0.7–1.0 pb. Unlike the QED background, the cut of $\theta_{J/\psi}$ only has a minor influence on σ_{QCD} because neither the CS nor CO contribution strongly depends on $\theta_{J/\psi}$ [16,22]. We, therefore, infer that with a suitable cut on $\theta_{J/\psi}$, the cross section of the QED background will be in the same order as that of the conventional QCD process. The calculation in Ref. [23] shows that the CO contribution mainly assembles in the kinematic end point region, while the CS contribution is distributed in a relatively flat manner in the whole $0 < p_{J/\psi} < 4.85$ GeV region. Thus to study the COM, people may also require $p_{J/\psi} > 3$ GeV in the measurement. Such a requirement will reduce the CS contribution by about 50%, but affects the CO contribution and QED background slightly. Based on the above analysis, we think further measurement of the $J/\psi + X_{\text{non-}c\bar{c}}^{N_{ch}\geq 0}$ production with a suitable cut on $\theta_{J/\psi}$ and $p_{J/\psi}$ will be helpful to understand the role of COM for J/ψ production in e^+e^- annihilation.

In this work, we calculate the QED background to the $J/\psi + X_{\text{non-}c\bar{c}}^{N_{ch}\geq 0}$ production by including the predominant contribution at α^3 and α^4 order. Higher order QED corrections are suppressed by QED coupling α, which is about 2 orders of magnitude smaller. In our calculation, we determine the coupling of effective vertices $\gamma^* \to \psi(2S)(J/\psi)$ and $\psi(2S) \to J/\psi + \pi\pi$ by fitting to experimental data and choose the extracted R-value [46] to describe the effective vertex of $\gamma^* q\bar{q}$. In this way, the theoretical uncertainties of these two background processes are removed. Besides the $\psi(2S) \to J/\psi + \pi\pi$ feed-down process, there are also feed-down contributions to the background from other higher charmonium states. They are all much suppressed too, because their branching functions to $J/\psi + X_{\text{non-}c\bar{c}}^{N_{ch}\geq 0}$ are very small. Therefore, the uncertainty of our calculation is small.

Recently, η_c hadroproduction was measured for the first time by the LHCb Collaboration [50]. With the help of heavy-quark spin symmetry, the LDMEs for η_c production can all be related to those for J/ψ production. It is found that the COM is challenged by the η_c hadroproduction data and only the CS contribution itself can explain LHCb measurements [51]. Studying J/ψ production at B factories can also deepen our understanding of the different roles of COM for J/ψ and η_c hadroproduction.

ACKNOWLEDGMENTS

We would like to thank ChangZheng Yuan and Chao-Hsi Chang for helpful discussion. Z. G. H. thanks the Theoretical Physics Center for Science Facilities (CAS) and Universitat de Barcelona for hospitality while part of this work was carried out. This work is supported by Key Research Program of Frontier Sciences, CAS, Grant No. Y7292610K1. The work of Z. G. H. was supported in part by the CSD2007-00042 Consolider-Ingenio 2010 program under Contract No. CPAN08-PD14, by the Spanish Grants from Ministery of Science and Education (Spain) No. FPA2007-66665-C02-01 and FPA2010-16963, and is supported by the German Federal Ministry for Education and Research BMBF through Grant No. 05H12GUE.

[1] G. T. Bodwin, E. Braaten, and G. P. Lepage, Phys. Rev. D **51**, 1125 (1995); **55**, 5853(E) (1997).
[2] N. Brambilla *et al.* (Quarkonium Working Group), CERN yellow report, CERN Report No. CERN-2005-005, 2005, p. 487; N. Brambilla *et al.*, Eur. Phys. J. C **71**, 1534 (2011).
[3] N. Brambilla *et al.*, Eur. Phys. J. C **74**, 2981 (2014).
[4] J. P. Lansberg, arXiv:1903.09185.
[5] B. Aubert *et al.* (*BABAR* Collaboration), Phys. Rev. Lett. **87**, 162002 (2001).
[6] K. Abe *et al.* (Belle Collaboration), Phys. Rev. Lett. **88**, 052001 (2002).
[7] B. Aubert *et al.* (*BABAR* Collaboration), Phys. Rev. D **72**, 031101 (2005).
[8] K. Abe *et al.* (Belle Collaboration), Phys. Rev. Lett. **89**, 142001 (2002); Phys. Rev. D **70**, 071102 (2004).
[9] P. Pakhlov *et al.* (Belle Collaboration), Phys. Rev. D **79**, 071101 (2009).
[10] K. Y. Liu, Z. G. He, and K. T. Chao, Phys. Rev. D **69**, 094027 (2004).
[11] P. L. Cho and A. K. Leibovich, Phys. Rev. D **54**, 6690 (1996); S. Baek, P. Ko, J. Lee, and H. S. Song, J. Korean Phys. Soc. **33**, 97 (1998).
[12] E. Braaten and J. Lee, Phys. Rev. D **67**, 054007 (2003); **72**, 099901(E) (2005); K. Y. Liu, Z. G. He, and K. T. Chao, Phys. Lett. B **557**, 45 (2003).
[13] Y. J. Zhang, Y. j. Gao, and K. T. Chao, Phys. Rev. Lett. **96**, 092001 (2006); Y. J. Zhang and K. T. Chao, Phys. Rev. Lett. **98**, 092003 (2007); Y. J. Zhang, Y. Q. Ma, and K. T. Chao, Phys. Rev. D **78**, 054006 (2008).
[14] B. Gong and J. X. Wang, Phys. Rev. D **77**, 054028 (2008); Phys. Rev. Lett. **100**, 181803 (2008); Phys. Rev. D **80**, 054015 (2009).
[15] G. T. Bodwin, D. Kang, T. Kim, J. Lee, and C. Yu, AIP Conf. Proc. **892**, 315 (2007); Z. G. He, Y. Fan, and K. T. Chao, Phys. Rev. D **75**, 074011 (2007).
[16] E. Braaten and Y. Q. Chen, Phys. Rev. Lett. **76**, 730 (1996).
[17] F. Yuan, C. F. Qiao, and K. T. Chao, Phys. Rev. D **56**, 321 (1997).
[18] S. Fleming, A. K. Leibovich, and T. Mehen, Phys. Rev. D **68**, 094011 (2003),
[19] J. X. Wang, AIP Conf. Proc. **1092**, 1 (2009).
[20] V. M. Driesen, J. H. Kuhn, and E. Mirkes, Phys. Rev. D **49**, 3197 (1994).
[21] Y. Q. Ma, Y. J. Zhang, and K. T. Chao, Phys. Rev. Lett. **102**, 162002 (2009).
[22] B. Gong and J. X. Wang, Phys. Rev. Lett. **102**, 162003 (2009).
[23] Y. J. Zhang, Y. Q. Ma, K. Wang, and K. T. Chao, Phys. Rev. D **81**, 034015 (2010).
[24] Z. G. He, Y. Fan, and K. T. Chao, Phys. Rev. D **81**, 054036 (2010).
[25] Y. Jia, Phys. Rev. D **82**, 034017 (2010).
[26] R. Li and J. X. Wang, Phys. Rev. D **82**, 054006 (2010).
[27] Z. G. He and J. X. Wang, Phys. Rev. D **81**, 054030 (2010); **82**, 094033 (2010).
[28] P. Artoisenet, J. M. Campbell, F. Maltoni, and F. Tramontano, Phys. Rev. Lett. **102**, 142001 (2009).
[29] C. H. Chang, R. Li, and J. X. Wang, Phys. Rev. D **80**, 034020 (2009).
[30] M. Butenschoen and B. A. Kniehl, Phys. Rev. Lett. **104**, 072001 (2010).
[31] M. Butenschoen and B. A. Kniehl, Phys. Rev. Lett. **107**, 232001 (2011).
[32] J. M. Campbell, F. Maltoni, and F. Tramontano, Phys. Rev. Lett. **98**, 252002 (2007).
[33] B. Gong and J. X. Wang, Phys. Rev. Lett. **100**, 232001 (2008).
[34] B. Gong and J. X. Wang, Phys. Rev. D **78**, 074011 (2008).
[35] E. Braaten and S. Fleming, Phys. Rev. Lett. **74**, 3327 (1995).
[36] B. Gong, X. Q. Li, and J. X. Wang, Phys. Lett. B **673**, 197 (2009).
[37] Y. Q. Ma, K. Wang, and K. T. Chao, Phys. Rev. Lett. **106**, 042002 (2011).
[38] M. Butenschoen and B. A. Kniehl, Phys. Rev. Lett. **106**, 022003 (2011).
[39] M. Butenschoen and B. A. Kniehl, Phys. Rev. D **84**, 051501 (2011).
[40] M. Butenschoen and B. A. Kniehl, Phys. Rev. Lett. **108**, 172002 (2012).
[41] K.-T. Chao, Y.-Q. Ma, H.-S. Shao, K. Wang, and Y.-J. Zhang, Phys. Rev. Lett. **108**, 242004 (2012).
[42] B. Gong, L. P. Wan, J. X. Wang, and H. F. Zhang, Phys. Rev. Lett. **110**, 042002 (2013).
[43] M. Butenschoen and B. A. Kniehl, Mod. Phys. Lett. A **28**, 1350027 (2013).
[44] T. Mannel and R. Urech, Z. Phys. C **73**, 541 (1997).
[45] J. Z. Bai *et al.* (BES Collaboration), Phys. Rev. D **62**, 032002 (2000).
[46] K. Nakamura *et al.* (Particle Data Group), J. Phys. G **37**, 075021 (2010).
[47] J. X. Wang, Nucl. Instrum. Methods Phys. Res., Sect. A **534**, 241 (2004).
[48] C. H. Chang, C. F. Qiao, and J. X. Wang, Phys. Rev. D **57**, 4035 (1998).
[49] Y. J. Zhang, B. Q. Li, and K. Y. Liu, arXiv:1003.5566.
[50] R. Aaij *et al.* (LHCb Collaboration), Eur. Phys. J. C **75**, 311 (2015).
[51] M. Butenschoen, Z. G. He, and B. A. Kniehl, Phys. Rev. Lett. **114**, 092004 (2015).